Supporting Information

CO_2 electroreduction to ratio-tunable syngas with Cu-In-Ag electrodes: from electronic structure regulation to mechanistic understanding

Jingui Ma[1, 2], Zean Liu[2], Xiaonan Liu[2], Mengxuan Kuang[1], Yuhong Lai[2], Feiyu Li[2], Yu Chen[2], Quan Shi[1], Yansheng Liu[2], Junwei Hou[2, *]

1 State Key Laboratory of Heavy Oil Processing, China University of Petroleum-Beijing, Beijing 102249, China

2 State Key Laboratory of Heavy Oil Processing, China University of Petroleum-Beijing at Karamay, Xinjiang 834000, China

*Corresponding author.
E-mail, Junweihou@cupk.edu.cn

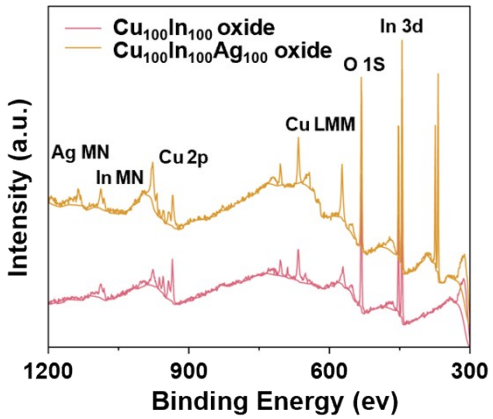

Fig. S1. XPS survey spectrum of the $Cu_{100}In_{100}Ag_{100}$ oxide and $Cu_{100}In_{100}$ oxide catalyst.

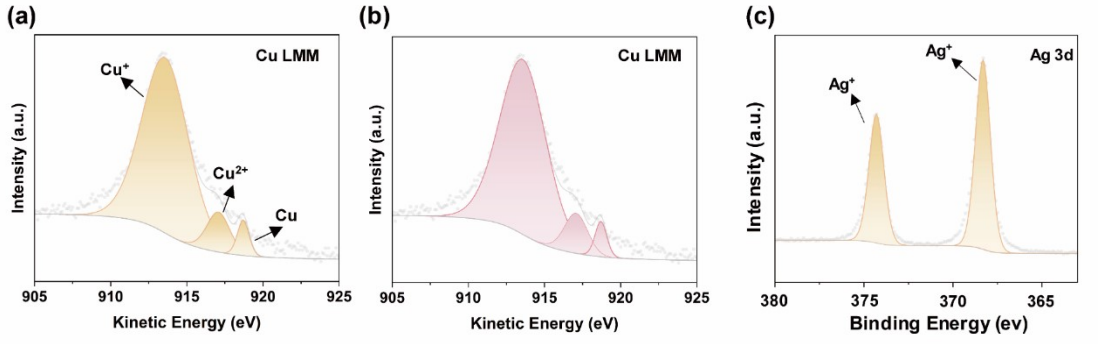

Fig. S2. XPS spectrum for Cu LMM of (a) $Cu_{100}In_{100}Ag_{100}$ oxide, (b) $Cu_{100}In_{100}$ oxide and (c) Ag 3d of the $Cu_{100}In_{100}Ag_{100}$ oxide.

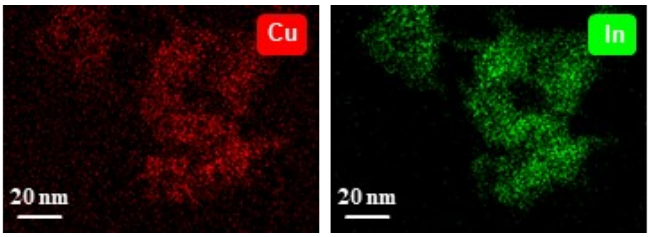

Fig. S3. EDX spectroscopy elemental mapping for Cu (red), In (green) of $Cu_{100}In_{100}$ oxide catalyst.

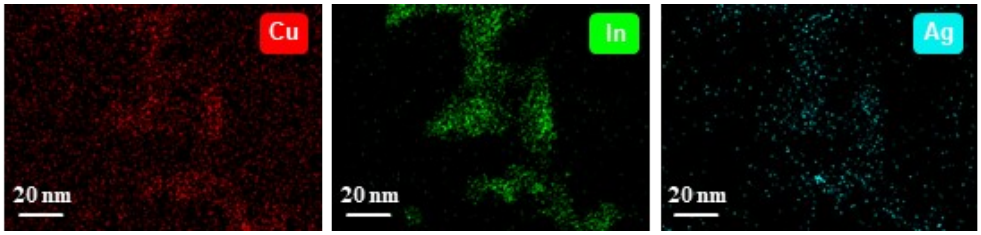

Fig. S4. EDX spectroscopy elemental mapping for Cu (red), In (green) and Ag (blue) of $Cu_{100}In_{100}Ag_{100}$ oxide catalyst.

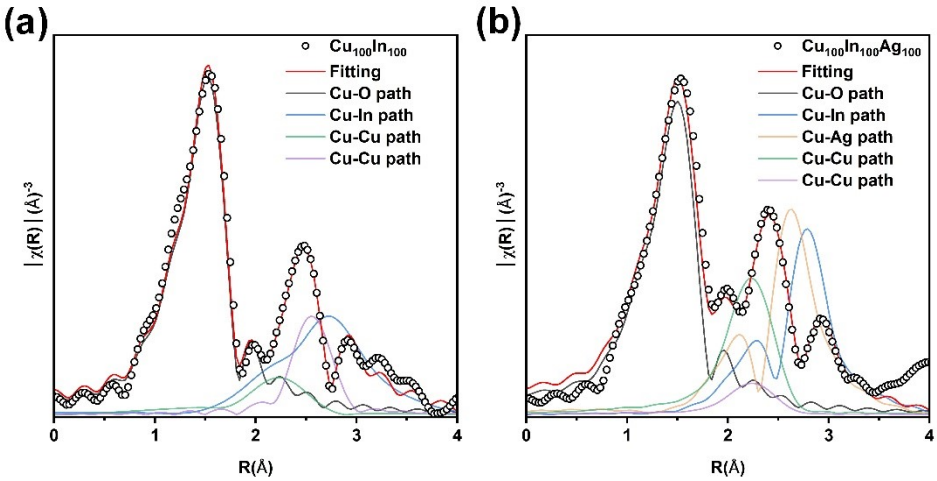

Fig. S5. Experimental and fitting spectrum of Cu K-edge in r space of (a) $Cu_{100}In_{100}$, (b) $Cu_{100}In_{100}Ag_{100}$

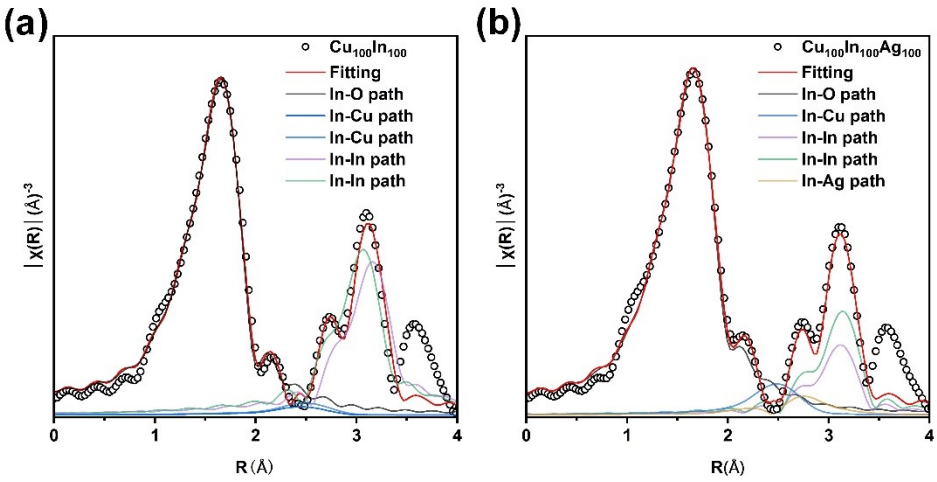

Fig. S6. Experimental and fitting spectrum of In K-edge in r space of (a) $Cu_{100}In_{100}$, (b) $Cu_{100}In_{100}Ag_{100}$

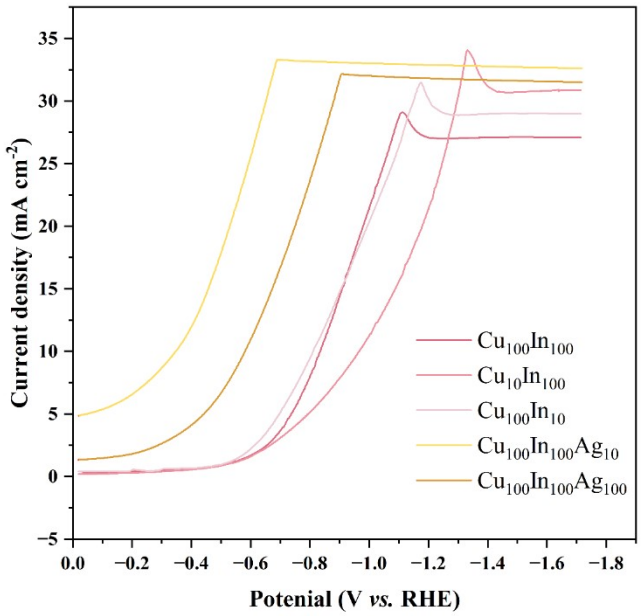

Fig. S7. LSV for different catalysts

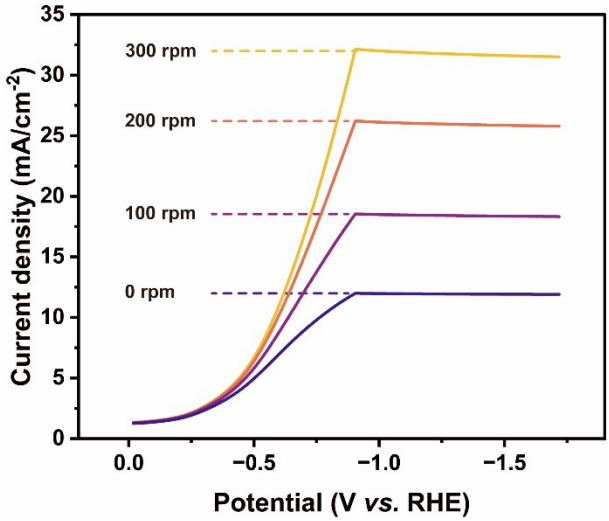

Fig. S8. LSV curves of the $Cu_{100}In_{100}Ag_{100}$ catalyst at different stirring speeds.

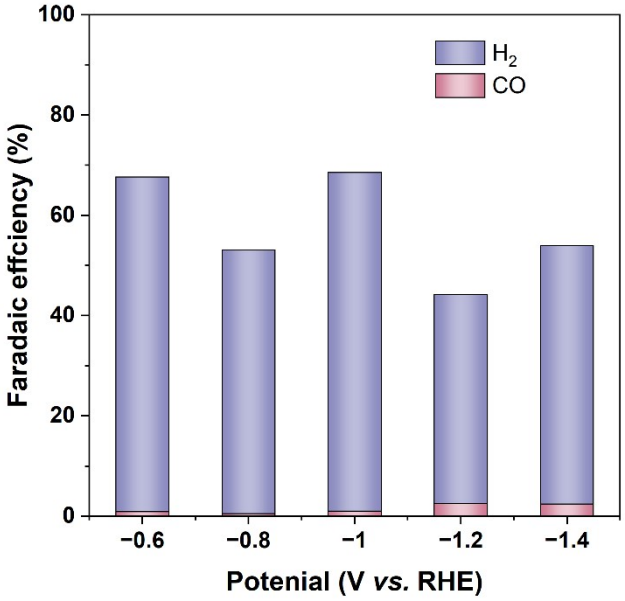

Fig. S9. FEs of CO and H_2 under different applied potentials over pure GDL in 0.1 M $KHCO_3$ electrolyte.

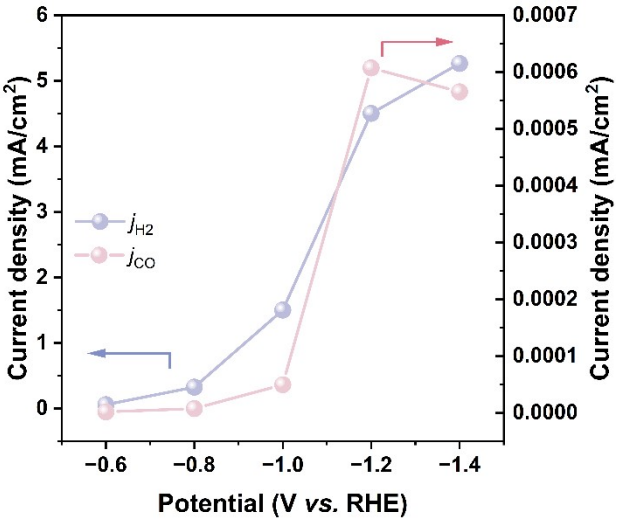

Fig. S10. partial current densities of CO and H_2 under different applied potentials over pure GDL in 0.1 M $KHCO_3$ electrolyte.

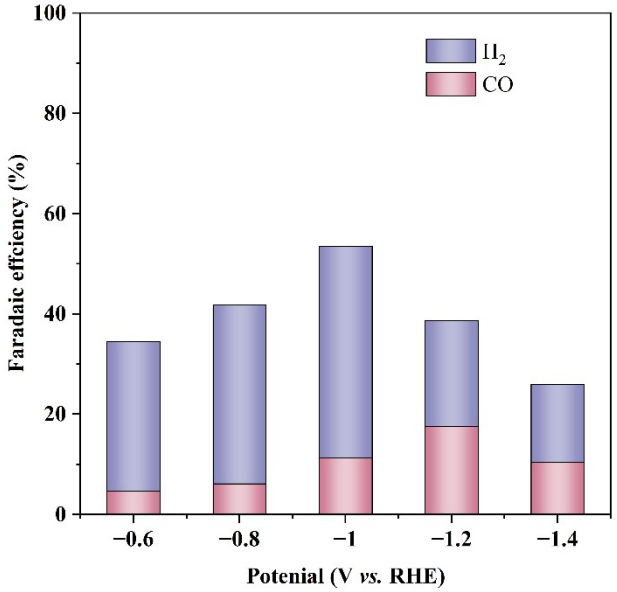

Fig. S11. FEs of CO and H_2 under different applied potentials over In NPs in 0.1 M $KHCO_3$ electrolyte.

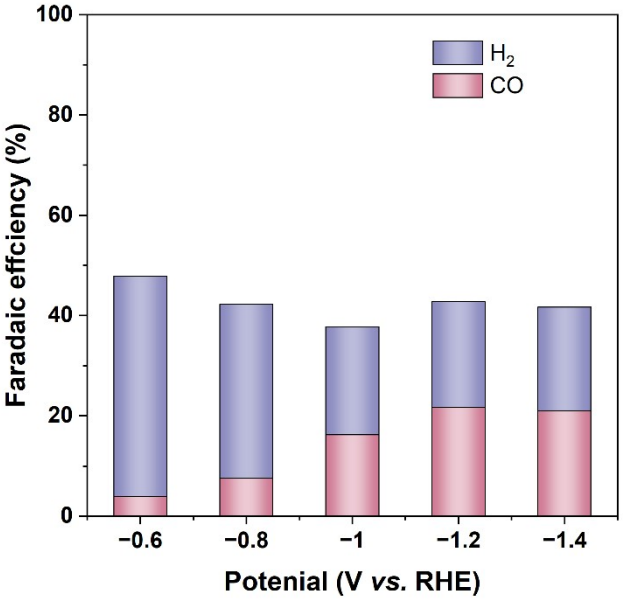

Fig. S12. FEs of CO and H_2 under different applied potentials over Cu NPs in 0.1 M $KHCO_3$ electrolyte.

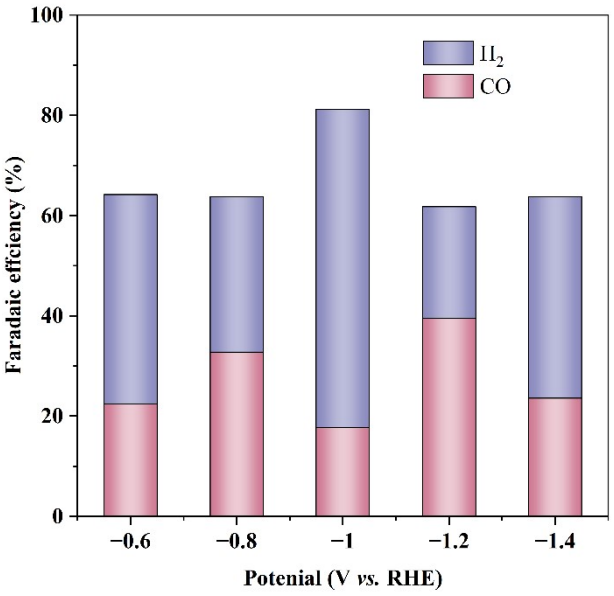

Fig. S13. FEs of CO and H_2 under different applied potentials over $Cu_{10}In_{100}$ in 0.1 M $KHCO_3$ electrolyte.

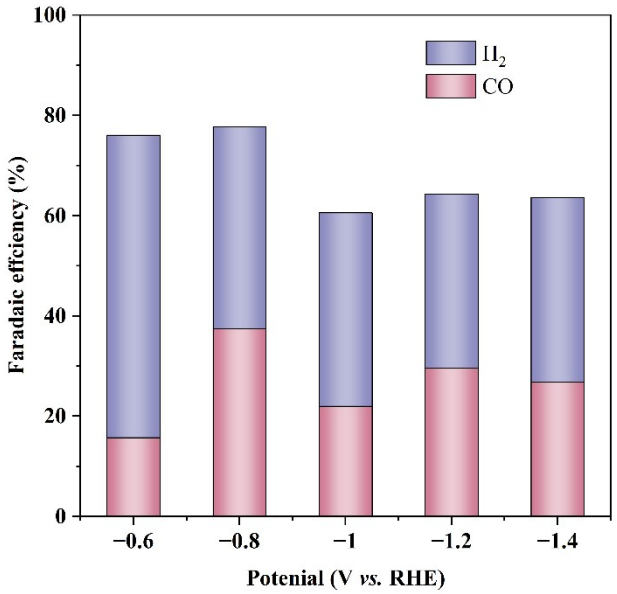

Fig. S14. FEs of CO and H_2 under different applied potentials over $Cu_{100}In_{10}$ in 0.1 M $KHCO_3$ electrolyte.

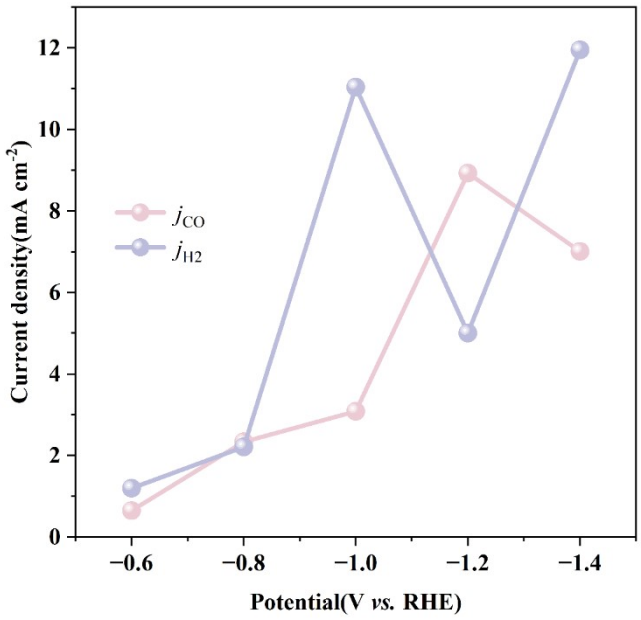

Fig. S15. Partial current densities of CO and H_2 under different applied potentials over $Cu_{10}In_{100}$ in 0.1 M $KHCO_3$ electrolyte.

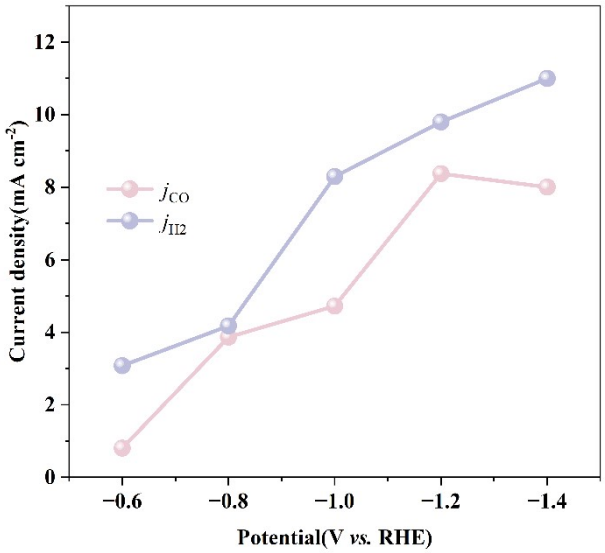

Fig. S16. Partial current densities of CO and H_2 under different applied potentials over $Cu_{100}In_{10}$ in 0.1 M $KHCO_3$ electrolyte.

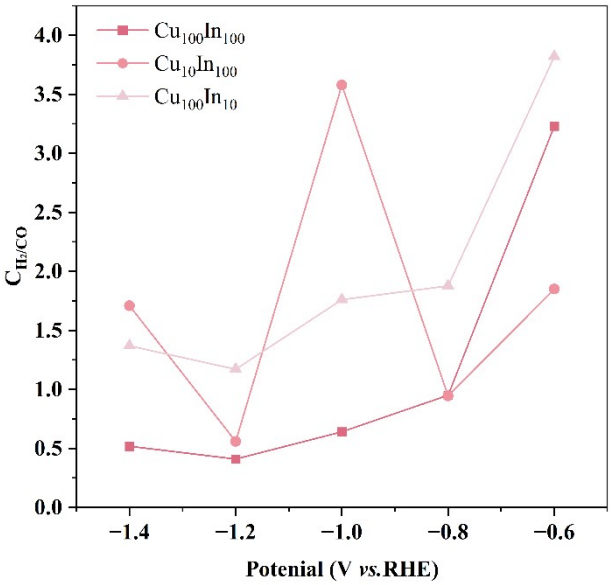

Fig. S17. Ratio of H_2/CO over different catalysts in 0.1 M $KHCO_3$ electrolyte.

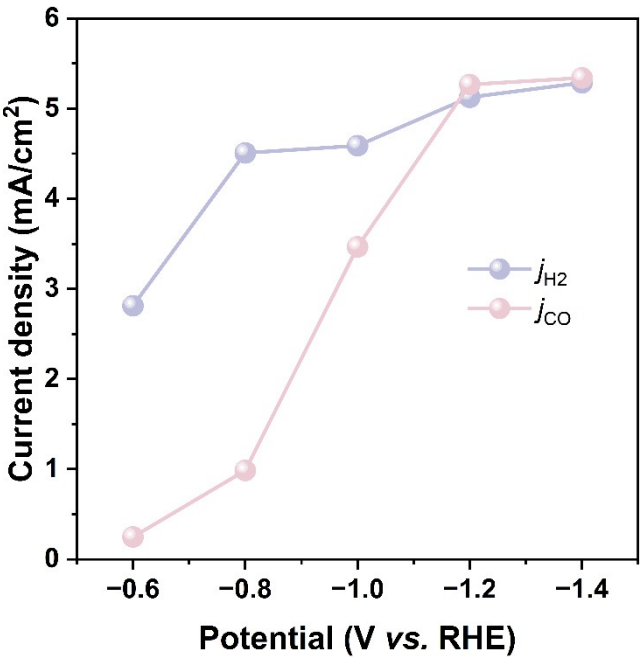

Fig. S18. Partial current densities of CO and H_2 under different applied potentials over $Cu_{100}Ag_{100}$ in 0.1 M $KHCO_3$ electrolyte.

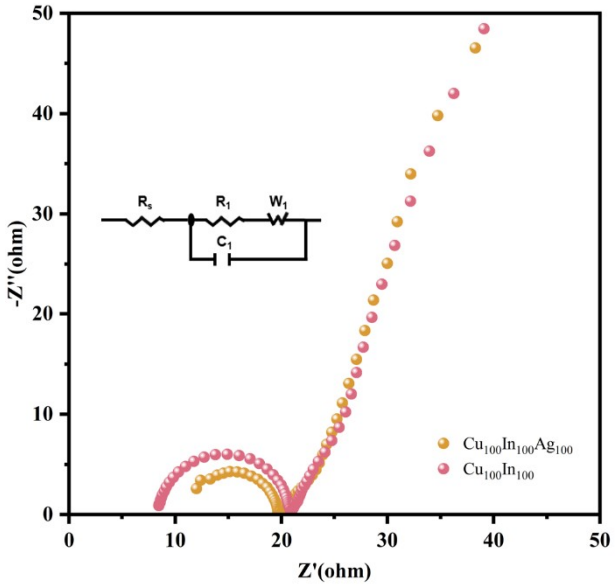

Fig. S19. EIS of the $Cu_{100}In_{100}Ag_{100}$ and $Cu_{100}In_{100}$ catalyst.

Fig. S20. FEs of CO and H_2 under different applied potentials over $Cu_{100}Ag_{100}$ in 0.1 M $KHCO_3$ electrolyte.

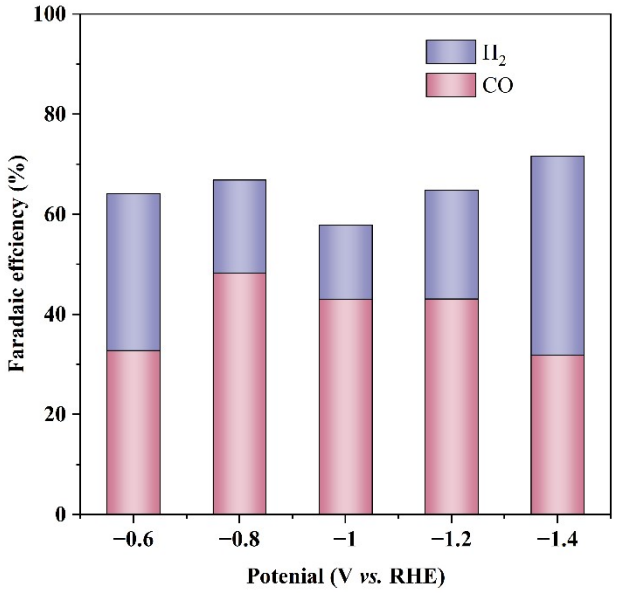

Fig. S21. FE of CO and H_2 under different applied potentials over $Cu_{100}In_{100}Ag_{10}$ in 0.1 M $KHCO_3$ electrolyte.

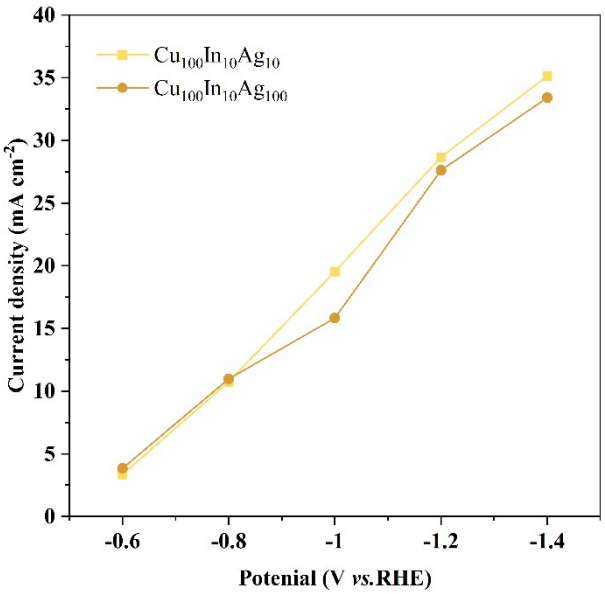

Fig. S22. Total current density over $Cu_{100}In_{100}Ag_{100}$ and $Cu_{100}In_{100}$ catalyst in 0.1 M $KHCO_3$ electrolyte.

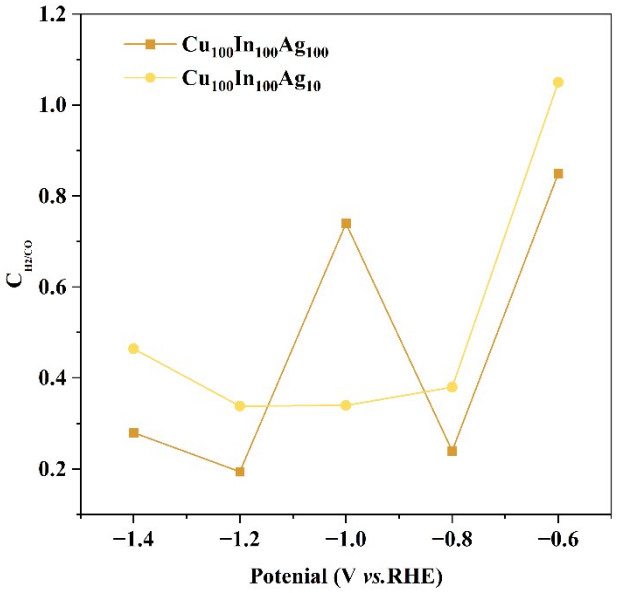

Fig. S23. Ratio of H_2/CO over different catalysts in 0.1 M $KHCO_3$ electrolyte.

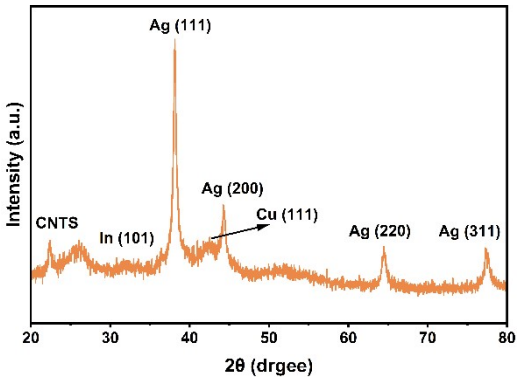

Fig. S24. XRD patterns of $Cu_{100}In_{100}Ag_{100}$ after an 8-hour stability test.

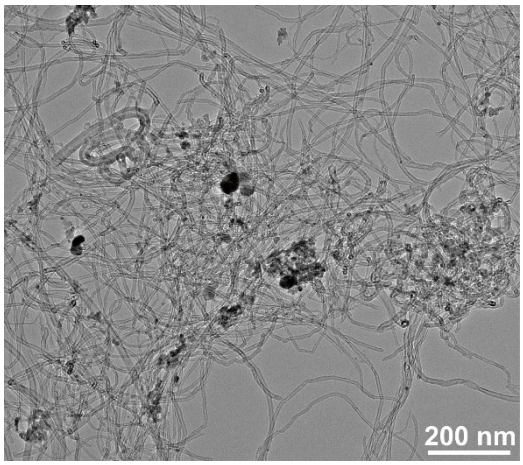

Fig. S25. HRTEM images of $Cu_{100}In_{100}Ag_{100}$ after an 8-hour stability test.

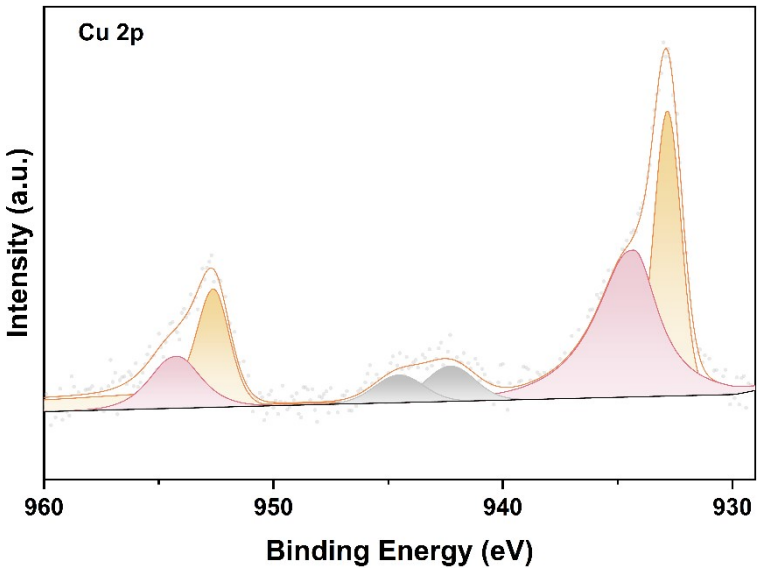

Fig. S26. Cu 2p XPS spectra of $Cu_{100}In_{100}Ag_{100}$ after an 8-hour stability test.

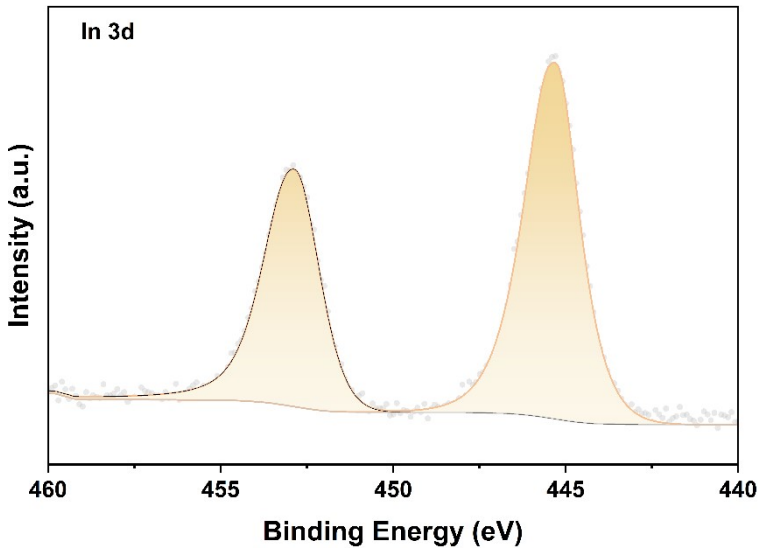

Fig. S27. In 3d XPS spectra of $Cu_{100}In_{100}Ag_{100}$ after an 8-hour stability test.

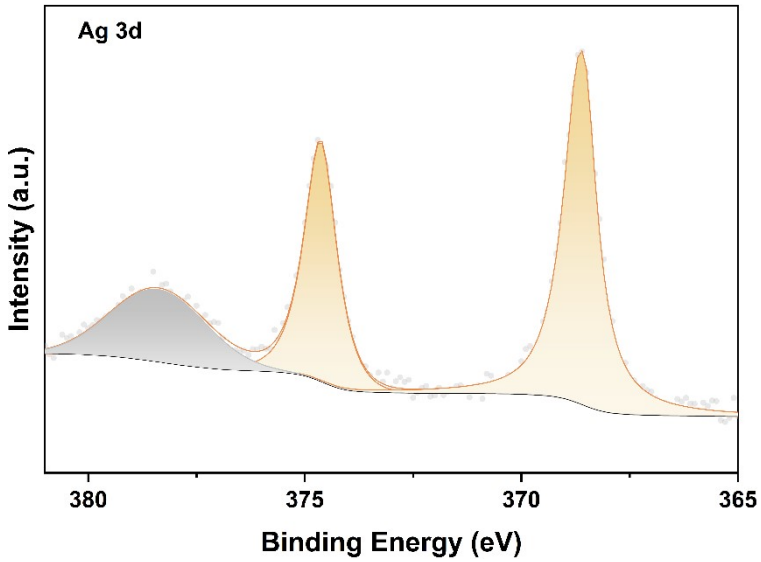

Fig. S28. Ag 3d XPS spectra of $Cu_{100}In_{100}Ag_{100}$ after an 8-hour stability test.

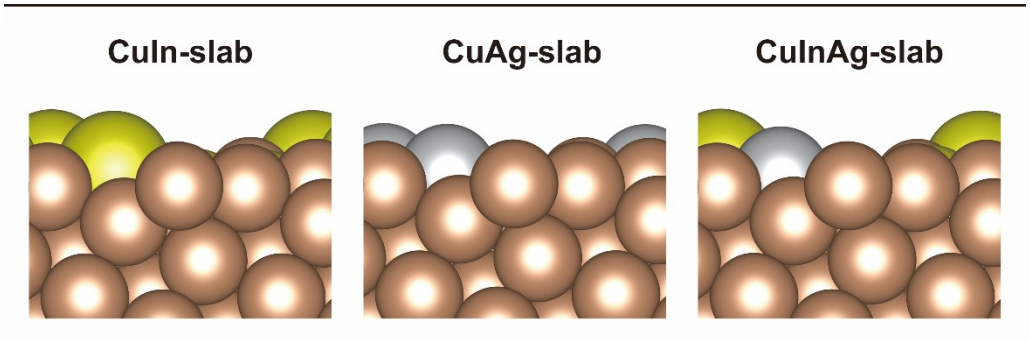

Fig. S29. Optimised structures of $Cu_{100}In_{100}$ and $Cu_{100}In_{100}Ag_{100}$.

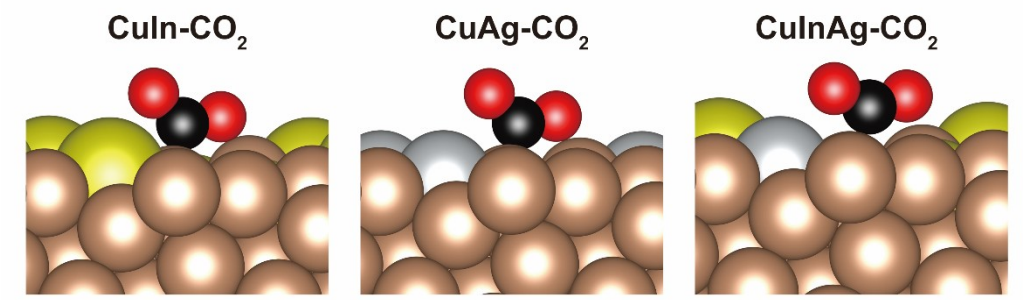

Fig. S30. Adsorption configurations of *CO_2 intermediates.

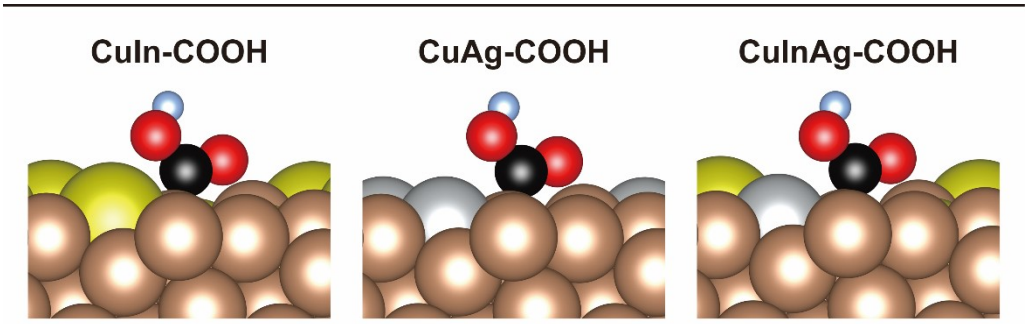

Fig. S31. Adsorption configurations of *COOH intermediates.

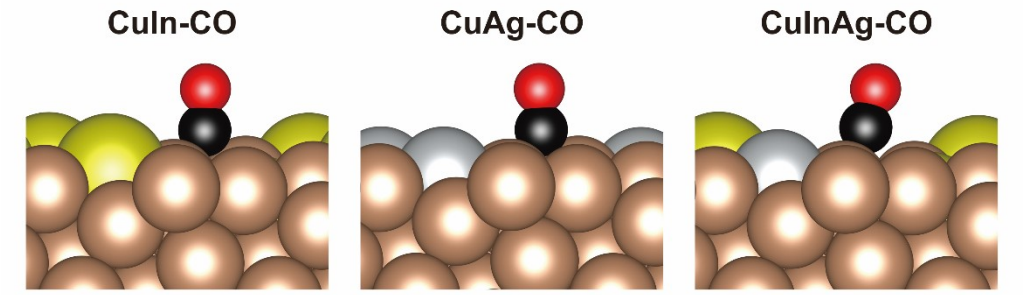

Fig. S32. Adsorption configurations of *CO intermediates.

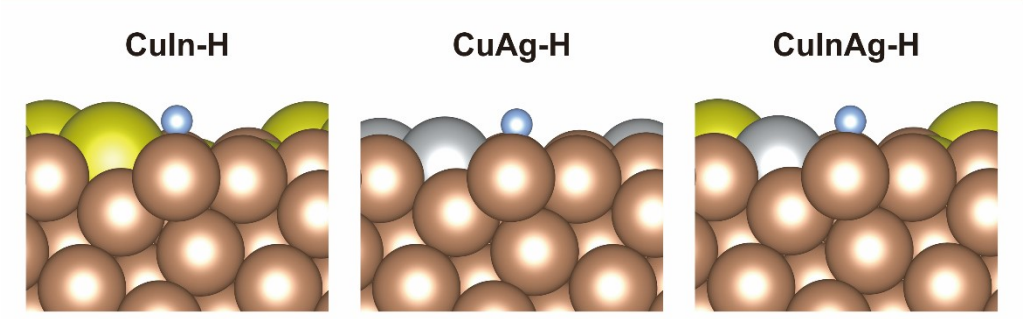

Fig. S33. Adsorption configurations of *H intermediates.

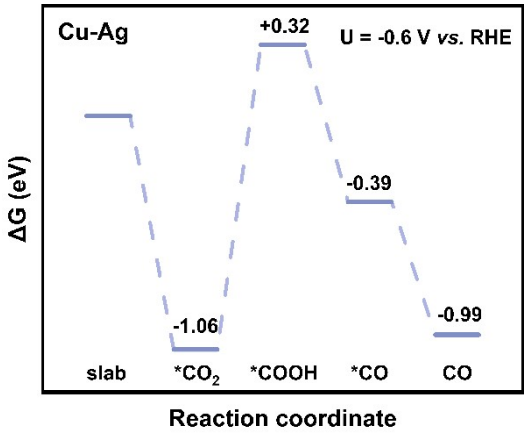

Fig. S34. Free-energy diagrams for CO_2 to CO on simulated Cu-Ag surfaces.

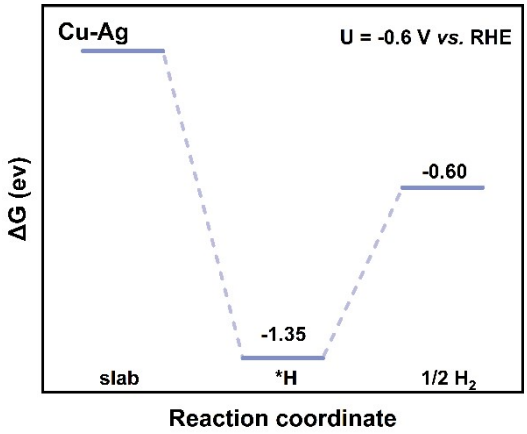

Fig. S35. Free-energy diagrams for H_2 evolution on simulated Cu-Ag surfaces.

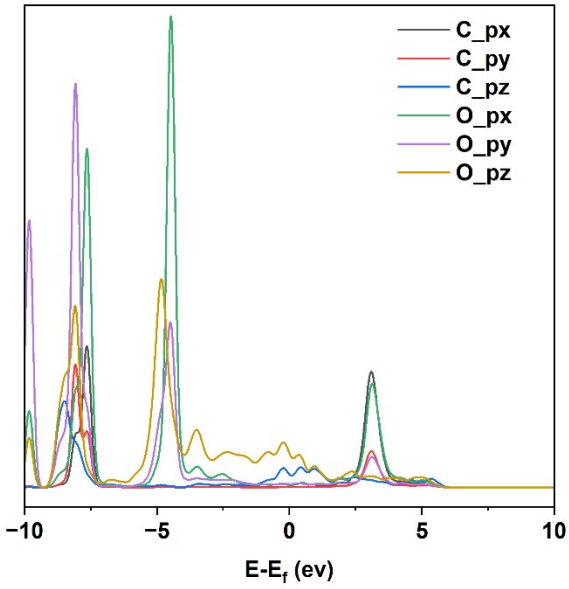

Fig. S36 The PDOS of CO_2 adsorbed on Cu-In-Ag surfaces.

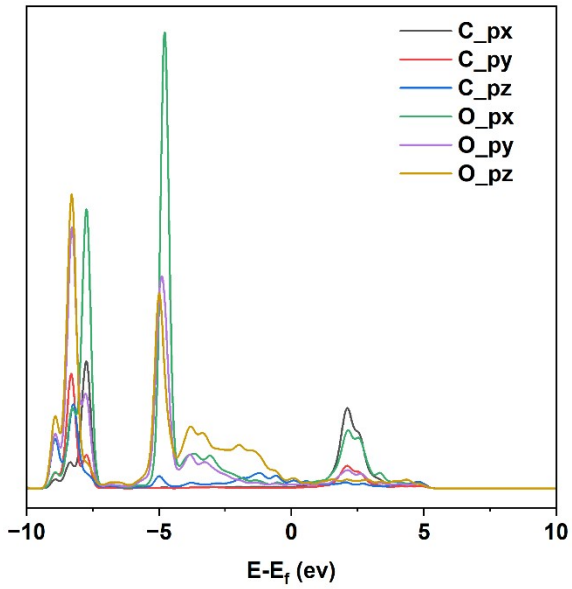

Fig. S37. The PDOS of CO_2 adsorbed on Cu-In surfaces.

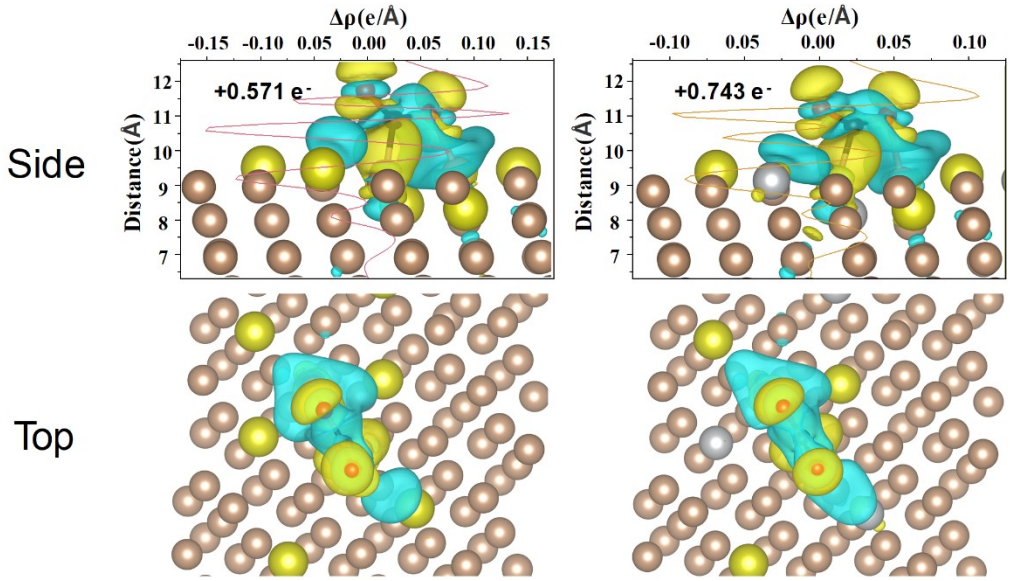

Figure S38. The PDOS and bader charge of CO_2 adsorbed on Cu-In and Cu-In-Ag surfaces.

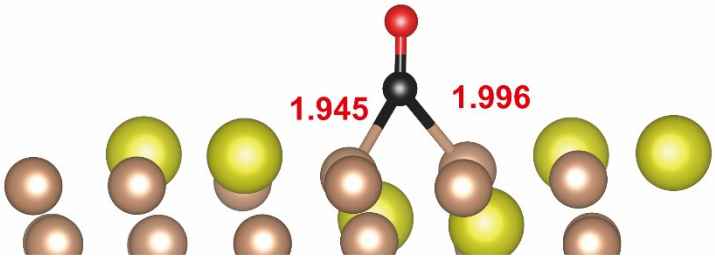

Fig. S39. structures of CO Adsorption on Cu-In surfaces.

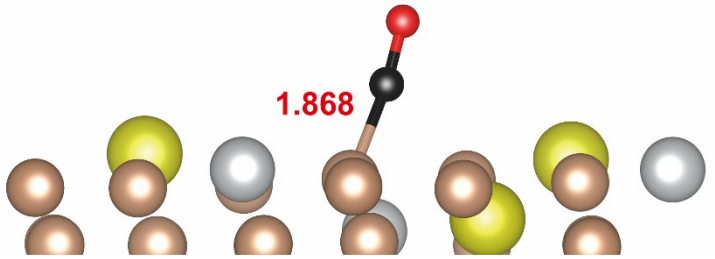

Fig. S40. structures of CO Adsorption on Cu-In-Ag surfaces.

Table S1. Electrochemical impedance parameters obtained by fitting the EIS data of $Cu_{100}In_{100}$ and $Cu_{100}In_{100}Ag_{100}$ electrodes

Equivalent Circuit Element	$Cu_{100}In_{100}$	$Cu_{100}In_{100}Ag_{100}$
R_S	8.45(±0.8%)	11.08(±2.4%)
R1	7.5(±0.9%)	7.6(±3.1%)
W1-R	97.84(±2.8%)	143.7(±2.0%)
W1-T	0.38(±2.7%)	20.31(±3.1%)
W1-P	0.69(±0.7%)	0.66(±0.7%)
C1	$2.14E^{-7}$(±2.3%)	$5.17E^{-8}$(±7.7%)

Table S2. The comparison of the syngas production performance for the multiple catalyst in H-cell reported in recent literature.

Catalyst	Electrolyte	Potential (vs. RHE)	j_{Total} (mA/cm^2)	Ratio H_2/CO	j_{H2} (mA / cm^2)	j_{CO} (mA / cm^2)	Ref.
$Cu_{100}In_{100}Ag_{100}$	0.1 M $KHCO_3$	−0.6 V	4.91	0.85	2.26	2.65	*This work*
AuZn-3/ZnO	0.1 M $KHCO_3$	−0.7 V	0.68	0.49	0.22	0.46	[52]
NiPC@FeNc	0.5 M $KHCO_3$	−0.6 V	4.36	0.61	1.65	2.71	[53]
Cu_4In_1/Bp-53	0.5 M $KHCO_3$	−0.6 V	4.60	1.60	2.83	1.77	[54]
R-Cu-500	0.1 M $KHCO_3$	−1.0 V	6.00	2	4.00	2.00	[55]
BPN-3Dp-CCE	0.1 M $KHCO_3$	−0.6 V	0.05	0.32	0.01	0.04	[56]